Large bent jets in the inner region of CSSs

F. Mantovani[1], **W. Junor**[2], **M. Bondi**[1], **W. Cotton**[3], **R. Fanti**[1,4], **L. Padrielli**[1], **G.D. Nicolson**[5], **and E. Salerno**[1]

[1] Istituto di Radioastronomia del C.N.R., Via P. Gobetti, I-40129 Bologna, Italy
[2] Institute for Astrophysics, University of New Mexico, NM, USA
[3] National Radio Astronomy Observatory, Charlottesville, USA
[4] Dipartimento di Fisica, Universitá degli Studi, Bologna, Italy
[5] Hartebeesthoek Radio Astronomy Observatory, Krugersdorp, South Africa

Abstract. The class of Compact Steep-spectrum Sources is dominated by double-lobed objects (70%). The remaining 30% are jet-dominated objects, with the jet brightened either by Doppler boosting or by interaction with the ambient media. We show that there is both observational and statistical evidence in favour of an interaction between jets and dense gas clouds. Such an interaction should happen in the Narrow Line Regions. The images of four CSSs observed by us with VLBI are also presented. These sources do show large bent jets in the first kpc from the nucleus.

Key words: galaxies: active – galaxies: jets – quasars: general – radio continuum: galaxies

1. Introduction

The class of Compact Steep-spectrum Sources (CSSs) has been discussed by many authors (e.g. Pearson et al. 1985; Fanti et al. 1990). It is now generally believed that CSSs are physically small objects with sub-galactic dimensions, whose structure and sizes are possibly affected by the ambient gas in the central regions of the parent optical objects. Double-lobed sources represent $\sim$ 70% of the objects in a sample of CSSs (Fanti et al. 1995) selected from the 3CR catalogue (Laing et al. 1983) and from the Peacock & Wall (1982) catalogue for a linear size < 15 kpc, spectral index $\alpha > 0.5$ (S$\propto \nu^{-\alpha}$) and radio power $\geq 10^{27}$ W Hz^{-1} at 178 MHz for the 3CR or $\geq 10^{26}$ W Hz^{-1} at 2.7 GHz ($H_0 = 100$km sec^{-1}Mpc^{-1} and $q_0 = 1$). Fanti at al. (1995) suggest that double-lobed CSSs represent the *young* ($\leq 10^6$ yrs) precursors of the larger double-lobed radio sources. The remaining 30% might represent a different population, made of sources where the jets are brightened either by Doppler boosting or by interaction with the ambient medium.

Send offprint requests to: Franco Mantovani
(fmantovani@ira.bo.cnr.it)

There are observational results that suggest a connection between radio source evolution and the CSS and GPS (Giga-Hertzed Peaked Sources) phenomena (see, for example, O'Dea et al. 1991; Stanghellini et al. 1992). These results also support the hypothesis that the CSS phenomenon results from expansion within the ambient environment of radio sources at intermediate and high redshifts. This may be due to the existence of a more dense ISM in the inner portions of host galaxies with CSSs. This density enhancement would influence the behaviour of the radio-emitting regions.

Generally speaking, the cores are often weak in CSSs, suggesting that if boosting is present, then jets and cores are misaligned with respect to the kpc-scale jets (Spencer 1994). Moreover, distorted structures on the milli-arcsecond scale are common in those CSSs which are quasars with strong jets.

In this paper we focus our attention on a sample of CSSs selected because of the large bends in the jets in their inner regions. We will consider whether the large misalignments are due to relativistic effects or produced by jet-cloud interactions in Narrow Line Regions. In the next section we will describe the sample, our observations of four of the selected sources and the source structures. We will then summarize the source parameters derived from the observations, and estimate the probability of the collision of a jet with dense gas cloud. Finally, we will discuss the results of our investigations.

2. The sample

We have used the images of sources classified as CSSs from the compilation by Dallacasa & Stanghellini (1990). From this, we have chosen a sub-sample using quite simple criteria. First, all the sources dominated by jet emission were selected. From this, a list of sources was chosen to include all the sources showing large bent jets on the sub-arcsecond scale. A bend in a jet is considered *large* when the jet major axis changes direction by an angle $> 50°$ ($\Delta PA > 50°$).

Such a value was adopted to avoid ambiguities in selecting candidates from the published images. These are due to the

Table 1. Observing information

Source	Array	Freq.	Term.	Obs.Date	Track.	Corr.
0548+165	B,S,J2,L,I,O,W	5 GHz	MK3-B	12May1995	12 hrs	MPIfR
	B,S,J1,L,O,W,K,H,G, VLBA	1.6 GHz	MK2	21Sep1992	04 hrs	CIT
1741+279	B,J2,L,I,O,W	5 GHz	MK3-B	14Sep1993	10 hrs	MPIfR
	B,J1,L,O,W,K,H,G, VLBA	1.6 GHz	MK2	21Sep1992	09 hrs	CIT
2033+187	B,J2,L,I,O,W	5 GHz	MK3-B	01Mar1994	10 hrs	MPIfR
	S,O,W,C,D,K,H,G, Hr,Fd,Ov	1.6 GHz	MK2	14Mar1986	08 hrs	CIT
2147+145	B,L,O,W	5 GHz	MK3-B	26Feb1994	11 hrs	MPIfR

Note: **B** Effelsberg, **C** Cambridge, **D** Defford, **Fd** Fort Davis, **G** Green Bank, **H** Hartebeestehoek, **K** Haystack, **Hr** Hat Creek, **J1** Jodrell-Lovell, **J2** Jodrell-MK2, **L** Medicina, **I** Noto, **O** Onsala85, **Ov** Owens Valley, **S** Simeiz, **W** Westerbork, **VLBA:** PT,KP,LA,BR,FD,NL,OV

uncertainty in determining the Position Angle (PA) of the jet major axis. We are also aware that the images were made from observations done using a variety of arrays and frequencies, some of which were inappropriate for our purpose. The selected sources are listed in Table 3 below. Observations of four of them by us are presented here.

2.1. The observations

The four sources (0548+165, 1741+279, 2033+187 and 2147+145) have been observed with VLBI at 1.6 GHz and 5 GHz using different arrays and recording systems. Calibration observations on largely-unresolved radio sources were made during each observing session along with the observations of the target source. Table 1 summarizes the observations. After the correlation process the bulk of the data reduction was done using the *AIPS* package. The sources have been imaged using both *AIPS* and *DIFMAP* (Shepherd et al. 1995).

The source parameters in Table 2 are as follows: – column 1: source name; column 2: observing frequency; columns 3,4,5: beam major axis, minor axis in mas and PA in degrees; column 6: r.m.s. noise in the map far from the source; column 7: component label; column 8,9,10: major axis, minor axis in mas and PA in deg of each component; column 11: component peak brightness in mJy/beam; column 12: component total flux density in mJy; column 12: component spectral index.

2.2. Description of sources

The four sources above plus the other sources listed in the following Table 3 are described briefly here:

3C43 (0127+233)

The VLA image from Pearson et al. (1985) shows a highly misaligned triple structure. The MERLIN map by Sanghera et al. (1995) shows that the northernmost component A in the EVN λ18cm image by Spencer et al. (1991) is likely to be the core. This is consistent with the λ50cm VLBI observations of Rendong et al. (1991). Spencer (1994) imaged 3C43 at λ18cm with MERLIN. That image shows a bridge of emission between the main components and the northern component. The jet is straight and collimated for the first 150 mas, then it changes PA by $33°$ and, after 75 mas the PA changes again by $60°$ pointing towards east. According to Junor et al. (in preparation) the central component is 3.6% polarized at 8.4 GHz with the VLA. The polarized intensity is sufficiently strong to provide an estimate of Rotation Measure, RM, of -1800 rad m^{-2} in the source's rest frame. The intrinsic magnetic field direction in the central component follows the curvature of the source faithfully.

3C99 (0358+004)

The radio source 3C99 has a triple structure on arcsecond scales. The outer components are located rather asymmetrically relative to the nucleus and have very different surface brightnesses (Mantovani et al. 1990). Along the major axis, 3C99 has an angular size of $\simeq 6$ arcsec and a linear size of $\simeq 21$ kpc. It is associated with an N galaxy which has been detected close to the central component (Spinrad et al. 1985). The central component is unpolarized in 8.4 GHz VLA observations (Mantovani et al. 1997) and it is likely to be the nucleus of 3C99. The VLBI image of the source at λ18cm shows that the central component consists of several blobs of emission with the two prominent ones being significantly misaligned with the overall axis of the source.

3C119 (0429+415)

An image of the source structure with an angular resolution of 5 mas is presented by Nan Ren-dong et al. (1991). Component A has an inverted spectral index and it is identified with the core of 3C119. The morphology of 3C119 is rather peculiar. The jet emerging from the core component is not well collimated. It contains several blobs of emission. The major axis PA changes direction by $55°$ to reach the component C, at about 40 mas from the core. From there, it changes direction several times to form an almost circular structure. The core has a radio luminosity which is $< 2\%$ of the source total luminosity at 5 GHz. Taylor et al. (1992) listed 3C119 among sources with very large Rotation Measures (RM=3400 rad m^{-2}). A number of possible explanations have been discussed in the paper by Nan Ren-dong et al. (1991) for the source's brightness distribution (e.g. rotational shear of the radio jet by an ambient rotating gaseous disk, precession in the nucleus, and the source expanding in a cavity

Table 2. Sources parameters

Source	Obs.	Beam			rms	C	De.Size			Flux	Dens.	α
	ν	maj	min	PA	noise		maj	min	PA	peak	total	
	MHz	mas	mas	deg	mJy/b		mas	mas	deg	mJy/b	mJy	
0548+165	1662	14	10	8	10	a	-	-	-	116	131	0.2
						j	-	-	-	62	162	
						b	20	9	15	693	1571	1.3
						c	-	-	-	16	18	
	4975	6	6		0.2	a	-	-	-	92.6	109.1	
						j	-	-	-	8.3	49.1	
						b	14	9	9	110.9	376.5	
						c	21	9	34	15.8	92.0	
1741+279	1662	12	9	–2	2.5	a	-	-	-	53	57	−0.3
						b	29	11	104	10	44	1.3
						c	36	9	110	6	25	1.8
						d	-	-	-	18	23	1.3
						e	13	8	7	77	178	1.4
	4960	8.5	5.7	79	0.12	a	4	2	69	75.9	82.9	
						b	13	12	108	3.3	10.7	
						c	6	2	172	2.3	3.5	
						d	16	11	72	18.5	42.7	
						e	12	6	29	18.5	42.7	
2033+187	1662	19	3	–9	0.7	a	8	4	164	303.2	499.2	1.2
						a_1	33	3	164	12.6	23.9	
						a_2	12	4	33	64.0	154.8	
						b	10	3	175	63.5	133.9	1.1
						c	–	–	–	13.6	14.4	
						d	10	5	168	80.3	193.2	1.2
	4960	9.7	4.8	65	0.07	a	7	5	71	94.8	136.0	
						b	7	1	79	33.1	38.6	
						d	7.3	4.4	68	10.6	12.6	
						d_1	–	–	–	29.9	41.5	
2147+145	4960	12.6	8.2	70	0.2	a	–	–	–	394.5	486.5	
						b	19	6	55	40.5	56.5	
						c	14	7	107	9.1	9.6	
						d	17	1	153	23.8	61.5	
						e	–	–	–	5.0	3.6	
						f	–	–	–	6.7	6.1	

in the interstellar medium), but those authors admit that they cannot reach a satisfactory conclusion.

3C147 (0538+498)

3C147 has been observed by several investigators; see, for example, the collection of images by Alef et al. (1990). Those authors have also observed 3C147 with 5 GHz VLBI over three epochs. The source shows an unusually-complex, nonlinear structure which varies with time. Superluminal separation of two components in the core region was observed also. New 8.4 GHz data (Alef, private communication) confirm a mildly-superluminal separation velocity of $v_{app} \sim 1.3c/h$. The jet is embedded in a diffuse emission region and shows a change in the projected orientation of its major axis of 90° at ~ 200 mas from the core. A VLA image at 1 GHz (van Bruegel et al. 1984) shows a weak component north to the main one in a position which is opposite to the jet respect to the core. 3C147 shows large RM's of -3144 and $+630$ rad m^{-2} in the rest frame of the source for the

main component and for the extension to the NNE respectively (Junor et al. submitted).

0548+165

On arcsecond scales, the source shows an asymmetric structure with a strong, unresolved component coincident with a quasar at z=0.474 and a much weaker secondary component about 3 arcsec to the north. The faint, extended component is weakly polarized. Most of the polarization comes from the main component. This source has a RM of 1934 rad m^{-2}. The polarized emission is also strongly depolarized between 15 GHz and 5 GHz (Mantovani et al. 1994).

The mas scale structure of 0548+165 from a full-track, global λ 18cm program is shown in Fig. 1. The source has a straight jet pointing west which changes direction dramatically 90° at ~ 80 mas from the core.

The de-rotated magnetic field is aligned parallel to the east-west direction (Mantovani et al. 1994) like the straight part at the beginning of the jet.
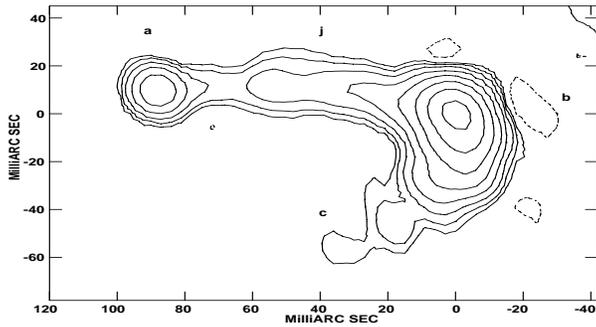
Fig. 1. VLBI image of 0548+165 at 18 cm. Contours are -4, 4, 8, 16, 32, 64, 128, 256, 512 mJy/beam. The peak flux density is 692.6 mJy/beam.

EVN observations at λ 6cm (Fig. 2) confirm the main structure seen at λ18cm. Fig. 2 also shows that the jet increases its width but it remains collimated and it seems to show a wiggling structure. The core is thought to be the easternmost component, since it has a flat spectrum. The detection of the secondary component about 3 arcsec north, suggests that either there is a counter jet or the VLBI jet bends back to the north.

3C287 (1328+254)

The image of 3C287 at λ6cm with 7 mas resolution shows a regularly curving jet-like structure; this bears some similarity to that in 3C119 (Fanti et al. 1989). The source brightness decreases smoothly along the curved jet. It is not clear where the core is located so we cannot add its parameters to Table 3. Fanti et al. 1989 suggest that the main component (A in their Fig. 3) is the possible site for the core. This is the most compact feature visible at λ6cm but it does have a spectral index of $\sim$0.5 between λ18cm and λ6cm (Nan Ren-dong et al. 1988).

1442+101 (OQ172)

This object is unresolved by MERLIN. The VLBI image shows a very compact source $\sim$ 70 mas in extent at λ18cm (Dallacasa et al. 1995). It has a core-jet structure with the core located in the northern part of the radio emission. The source shows a bend in the jet major axis PA of 90° at a separation of $\sim$ 15 mas. 1442+101 has a redshift of 3.544 and a very high integrated RM of 22400 rad m^{-2} in the source's rest frame (Taylor et al. 1992). Recent VLBA observations at 5 GHz by Udompresert et al. (1997) indicate that the RM is 40,000 rad m^{-2} in the rest frame of the quasar. At 10 mas from the nucleus the RM falls to less than 100 rad m^{-2}. The very high RM is found near to the core; it is likely that this is not associated with material which could influence the bending of the jet.

1629+680

This source was observed at λ13cm and λ3.6cm (Dallacasa et al. 1997). The X-band image shows a straight jet $\sim$ 30 mas long. The S-band image shows a mild bend in the jet which finally changes the direction of the axis by 90° at 100 mas from the core.

1741+279

The VLA map at 8.4 GHz of 1741+279 shows two bright components roughly aligned E-W, a wiggling jet 5 arcsec long aligned N-S to the north of the two bright components and a region of
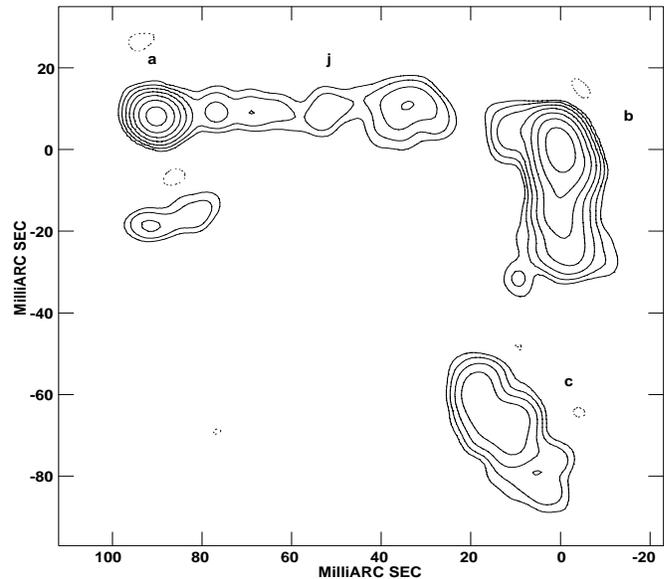
Fig. 2. VLBI image of 0548+165 at 6 cm. Contours are -1, 1, 2, 4, 6, 8, 16, 32, 64 mJy/beam. The peak flux density is 110.9 mJy/beam.

weak emission 4 arcsec to the south-south-east. The two compact components have about 5% of the total polarized emission at 8.4 GHz (Mantovani et al. 1997). The magnetic field is parallel to the curved line joining the two components, changing direction smoothly by an angle of $\sim$ 90°; this suggests that there is a bend in the emitting region. The VLBI λ18 cm and λ6 cm maps, Figs. 3 and 4 respectively, show several knots along the axis between these two components. The eastern component is the nucleus (it has an inverted spectrum) and the western one shows an elongation north-south. When compared with the λ3.6 cm VLA image, it is possible to imagine that this elongation is the location of a sharp bend or cusp in the jet's apparent path.

2033+187

This source is unresolved by the VLA A-array at 15 GHz (angular size < 0.05 arcsec) and is unpolarized. We present two VLBI images here. The first was obtained with a Global array at λ18 cm (Fig. 5); the second with the EVN at λ6 cm (Fig. 6). In these images, we see a straight jet and a dramatic bend at a small distance, 40 mas, from component 'a'. Note that component 'a' is the brightest feature in 2033+187 at both frequencies and shows a steep spectral index (α = 1.2). The position of the core is unknown. The resolution in the north-south direction is insufficient to resolve the westermost component at λ18 cm which has a low brightness region of emission extending south. The λ6 cm image shows a linear morphology from component 'a' to 'd', where the jet changes direction sharply.

2147+145

VLBI observations of 2147+145 were made for the first time by Cotton et al. (1984) at λ18 cm. That image shows a core-jet structure with the major axis PA of 45°. Recent VLA images of 2147+145 made at 8.4 and 15 GHz, when compared with the previous observations by Cotton (1983), show that the total flux

Table 3. Source parameters.

Source	ref	Sep. mas	Sep. pc	ΔPA deg	z	O.I.	$RM \times (1+z)^2$ rad m^{-2}	ref
0127+233 3C43	a	225	780	93	1.459	Q	−1088	1
0358+004 3C99	b	15	46	60	0.425	G	0	2
0429+415 3C119	c	39	142	55	1.023	Q	3400	3
0538+498 3C147	d	200	664	90	0.545	Q	−3144/630	4
0548+165	e	80	253	90	0.474	Q	1934	5
1328+254 3C287	f			58	1.055	Q	−	
1442+101 OQ172	g	15	39	90	3.531	Q	22400	3
1629+680 4C68.18	h	76	226	66	2.475	Q	−	
1741+279 B2	e	300	862	84	0.372	Q	−148/−279	2
2033+187	e	40	129	80	(0.5)	−	n	2
2147+145	e	23	75	90	(0.5)	−	n	2

Note – References - column 2 -: a. Spencer at al. (1991); b. Mantovani et al. (1997); c. Nan Ren-dong et al. (1991); d. Alef et al. (1990); e. this paper; f. Fanti et al. (1989); g. Dallacasa et al. (1995); h. Dallacasa et al. (1997). - column 9 -: 1. Junor et al. (in preparation); 2. Mantovani et al. (1997); 3. Taylor et al. (1992); 4. Junor et al. (1997); 5. Mantovani et al. (1995).
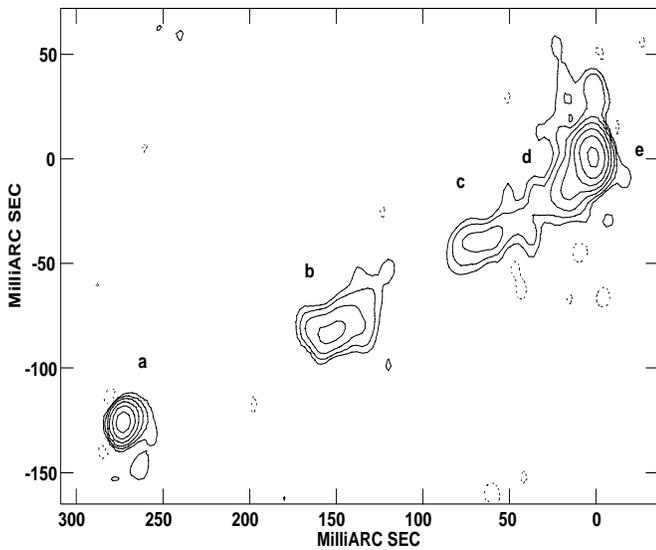
Fig. 3. VLBI image of 1741+279 at 18 cm. Contours are -1, 1, 2, 4, 8, 16, 32, 64 mJy/beam. The peak flux density is 77.3 mJy/beam.
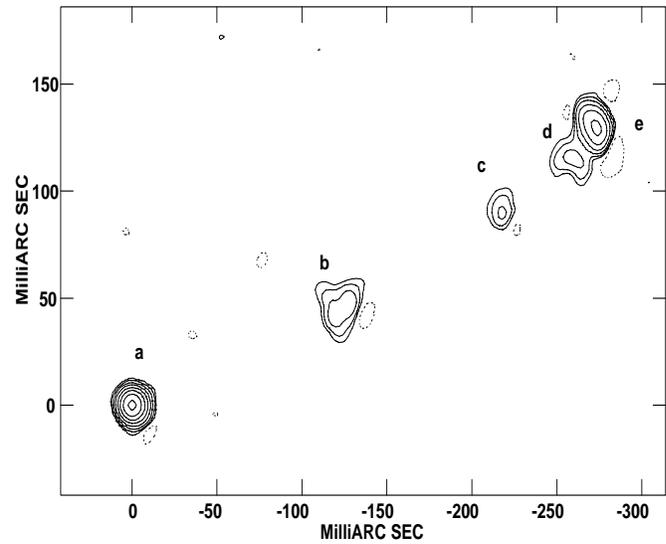
Fig. 4. VLBI image of 1741+279 at 6 cm. Contours are -0.5, 0.5, 1, 2, 4, 6, 8, 16, 32, 64 mJy/beam. The peak flux density is 75.9 mJy/beam.

density at 15 GHz has increased by ∼13%. In addition, a new component is found north of the core in PA −40°, separated by 0.35 arcsec (Mantovani et al. 1997). This component lies in a direction which differs by more than 80° from that found for the jet in the λ18 cm VLBI map of Cotton et al. (1984). The VLBI source can be modelled by four Gaussian components that lie along a path which bends smoothly towards north. It is reasonable to expect that the jet continues with an increasingly pronounced bend to allow the flow to reach the component to the north.

The EVN observations of 2147+145 at λ6 cm (Fig. 7) have produced an image that shows a core-jet structure which, at first sight, agrees with the λ18cm image of Cotton (1984). A sharp bend in the jet occurs at ∼40 mas from the core. The flow changes direction by ∼ 90° and a couple of weaker components

are detected further north. The component 'a', possibly the core, has a steep spectrum. The spectral index ranges from 0.38 (peak emission) to 0.7 (total emission) between λ18cm and λ6cm.

2.3. Summary of source parameters

Some of the parameters for the overall mas-scale structure that can be derived from the available images of these sources are summarized in Table 3. The table contents are as follows: – column 1: name; column 2: references for the images; column 3: separation (in milliarcsecond) between the core and the first large bend in the jet; column 4: linear separation, assuming $H_0 = 100 \, \mathrm{km \, sec^{-1} Mpc^{-1}}$ and $q_0 = 1$; column 5: difference in the jet PA before and after the bend (in degrees); column 6: redshift; column 7: optical identification; column 8: Rotation Measure in rad m^{-2} corrected by the redshift. The symbol '–'
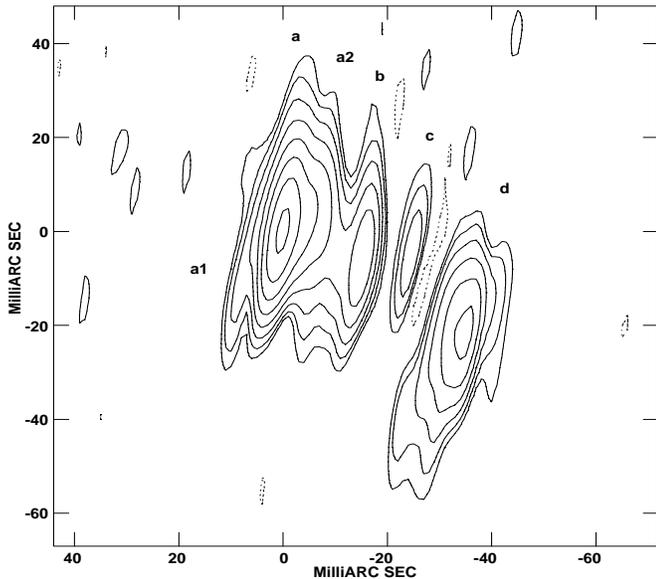
Fig. 5. VLBI image of 2033+187 at 18 cm. Contours are -2, 2, 4, 8, 16, 32, 64, 128, 256 mJy/beam. The peak flux density is 303.2 mJy/beam.

Fig. 6. VLBI image of 2033+187 at 6 cm. Contours are -1, 1, 2, 4, 8, 16, 32, 64 mJy/beam. The peak The peak flux density is 94.8 mJy/beam.

means measurements are unavailable. The symbol 'n' means polarization was not detected; column 9: references for RMs.

Because of the selection criteria adopted, the sources listed in Table 3 are characterized by the presence of bright jets. The change in the jet major axis Position Angle has a mean value of $\Delta PA = 78°$. The emission from the core compared to the total source emission is weak ($<$ 1%) in 3C43, 3C99, 3C119 and 3C147. However, it is strong ($>$ 5%) in 0548+165, 1629+680, 1741+279 and 2147+145. In two cases, namely 3C287 and 2033+187, it is still unclear where the core is located. It is worthwhile mentioning that all of the sources in Table 3 have been identified with quasars — with the exception of 3C99, which has been classified as an N-galaxy. Note, too, that the sources 2033+187 and 2147+145 are associated with unusually-faint optical objects (Cotton et al. 1989).

The sites where the bends occur are very close to the cores of the sources. The angular separation from the core to that location ranges between 15 and 300 mas, which corresponds to a linear separation of 40–900 pc, which is well inside the respective Narrow Line Regions (NLRs).

In general, most of the sources have a **very** high Rotation Measure. The sources are too compact to allow arcsecond-scale RM images. Those sources which are not polarized are also the most compact among those listed; this might be interpreted as due to large changes in the magnetic field direction within the angular resolution of the synthesized beam. In such cases, VLBI polarimetry is required; see, for example, the observations of 1442+101 (Udomprasert et al. 1997)

3. Statistical consideration

The list of CSSs compiled by Dallacasa & Stanghellini (1990) contains ∼130 objects. About 30% of these (i.e. ∼ 39 objects)
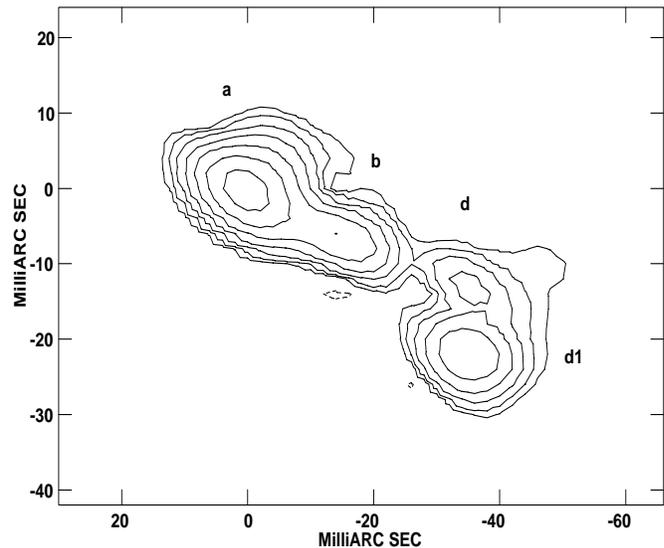
are dominated by the emission from the jet structure. Table 3 contains 11 objects with strongly bent jets, which represents about 30% of this sub-sample of CSSs (or ∼8% of the total number of CSSs) which is a reasonably-significant number.

If we consider instead the complete sample of CSSs defined by Fanti et al. (1995) which contains 43 objects then five of them, i.e. ∼11%, are listed in Table 3. This confirms that a strongly-bent jet is a noticeable phenomenon among this class of object.

As a comparison sample, we have taken the compilation of 293 Flat-Spectrum Radio Sources constructed by Taylor et al. (1996) which gives a complete Flux Density Limited VLBI sample. Following Wilkinson (1995), 82% of objects in this sample are classified as asymmetric core-jet sources. We have found only 4 sources in this sample which exhibit a bent jet fitting the selection criteria, and on the same scales, that we have used for the CSSs listed in Table 3. This number represents less than 2% of the objects in the complete sample and is much less than that found for the CSS complete sample. This last number should be treated with some care, however. The observations of the Flat Spectrum Sample were made with a high resolution VLBI array, limited in sensitivity by the snap-shot observing strategy adopted. Deeper observations might change the number of objects with large bent jets.

However, we consider the large fraction of objects with a strongly-bent jet among CSSs as an indication that the propagation of the jet is strongly affected by the ambient medium.

Let us calculate the probability of a collision between the jet and the dense gas clouds in the NLR surrounding the radio source. The outer gas is characterized by temperature of $\sim 10^4~K$, a particle density of $\sim 10^4~cm^{-3}$ and by a filling fac-
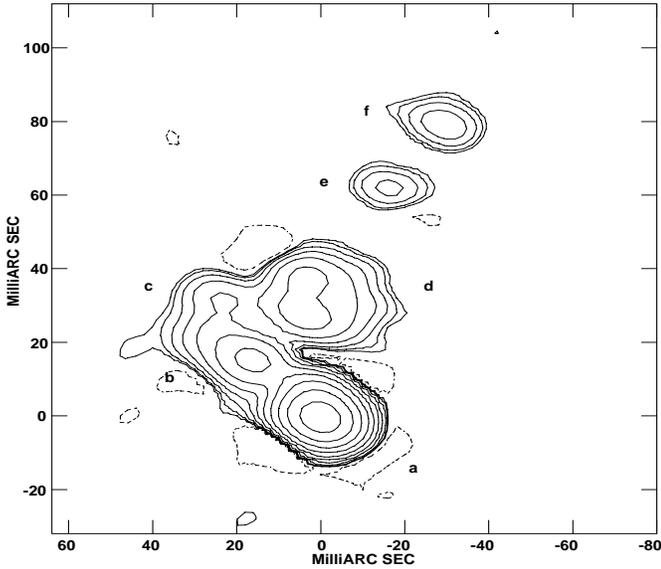
Fig. 7. VLBI image of 2147+145 at 6 cm. Contours are -0.6, 0.6, 1, 2, 4, 8, 16, 32, 64, 128, 256 mJy/beam. The peak flux density is 394.5 mJy/beam.

tor $\phi \leq 10^{-4}$ (McCarthy 1993). The number of clouds, B, that the jet will encounter in a distance L is given by:

$$B = d^2 \times L \times n = d^2 \times L \times \frac{N}{L^3} = \frac{d^2}{L^2} \times N \qquad (1)$$

where N the total number of clouds, L is the size of a Narrow Line Region, d the diameter of a cloud, and n is the cloud spatial density N/L^3. The diameter d and the density n of these dense gas clouds in active galaxies with $z \geq 0.1$ is still uncertain. The term B can be expressed more appropriately in terms of the filling factor.

The radio jet propagates in a single preferred direction; thus we are interested in determining the linear filling factor ϕ_l, which is defined as:

$$\phi_l = \frac{B \times d}{L} = \frac{d^2}{L^2} \times N \times \frac{d}{L} = \frac{d^3}{L^3} \times N \qquad (2)$$

The term on the right is, by definition, the *volume filling factor* ϕ_v. Such an expression is valid if the jet diameter is $< d$, the cloud's diameter. From this, one can derive $n = \phi_v/d^3$ and B can be calculated as:

$$B = d^2 \times L \times \frac{\phi_v}{d^3} = \frac{L\phi_v}{d} \qquad (3)$$

To estimate B, we have adopted the following values: (a) the linear size L of the NLRs can be taken to be in the range 1–10 kpc. This range is suggested by the bends which occur inside the first kpc from the core and from the fact that we are dealing with CSSs whose linear size cannot exceed 15–20 kpc by definition; (b) the filling factor ϕ_v is 10^{-4}. However, from the luminosity in strong lines like Hβ in the NLR ($10^{39} - 10^{42}$ ergs s^{-1} in Seyfert 2s) and electron density of 10^3 cm^{-3}, the

filling factor can reach values as large as 10^{-2} (see, for example, Peterson 1997); (c) In nearby AGN, the NLRs are often partially resolved by the observations and the inferred sizes are generally ≥ 100 pc. This gives an upper limit to the diameter d for a cloud. In our own Galaxy, dense clouds are characterized by sizes of 1–10 pc (Cowie & Sangaila 1986; Cox & Reynolds 1987). Thus the cloud diameters can be taken to be in the range 10–100 pc. Moreover, from the VLBI observations we see that the jets are not resolved in a direction transverse to the major axis, with an angular resolution of ~ 7 mas (about 10 pc for $z = 0.5$).

From these considerations, and assuming that the jet diameter is $< d$, then B will fall in the range 0.1–0.01. This last value is not just the number of collisions between the radio jet and the dense gas cloud in a CSS. It also represents the fraction of sources which suffer for such an interaction. Here we wish to stress that the chances of such a collision are not very small.

The Dallacasa & Stanghellini (1990) list of CSSs contains more than one hundred objects. The percentage of CSSs which show large bends in the propagation direction of the radio jet is a number which is roughly in agreement with the value derived here. The above considerations also indicate that the the probability of multiple bends is quite small.

4. Discussion

Sub-arcsecond resolution VLBI maps of CSSs often show that these sources have strongly-distorted structures with recognizable jet-like features (Fanti et al. 1986; Spencer et al. 1991), consistent with strong dynamical interactions between the jets and the ambient media. Although the largest distortions are often seen in sources dominated by jets, and there are suggestions that this might at least partly be due to projection effects (e.g. Spencer 1994), there are clear indications that intrinsic distortions due to interactions with a possibly-dense inhomogeneous gaseous environment play an important role. For example, some of the most distorted and complex structures are found in objects with very weak cores, as in the quasars 3C43 and 3C119. Such objects should be inclined at large enough angles to the line of sight that projection effects are not very significant. Generally speaking, CSSs usually show very weak cores compared to the jet emission while in superluminal sources the Doppler boosted cores are the components with the more dominant emission. Moreover, the only CSSs known so far which exhibit superluminal separation between two components, thus implying a small angle of inclination to the line of sight, are 3C147 ($v_{app} \sim 1.3c/h$; Alef et al. 1990) and 3C138 ($v_{app} \sim 5c/h$; Cotton et al. 1997). In addition to the distorted structures, an increased asymmetry in the location of the outer components also suggests that the components are evolving through a dense asymmetric environment in the central regions of these galaxies (Sanghera et al. 1995; Saikia 1995). Such an asymmetry between the mas structure and the arcsec structure is present where an arcsec structure is detected for sources in Table 3.

Most CSSs show low ($\sim 1\%$) percentage polarizations at or below 5 GHz (Saikia 1991; Saikia, Singal & Cornwell 1987). The median polarization, however, increases with frequency,

(van Breugel et al. 1992; Saikia 1995) suggesting that the polarimetric behaviour is due to Faraday depolarization. This pattern is consistent with the observation of Garrington and Akujor (1996) that smaller sources show stronger depolarization. A number of sources with very high Rotation Measures in the range of several thousands of rad m^{-2} are also CSSs. Most of the sources in Table 3 follow this trend having large depolarization and do have rather large RMs.

Sub-arcsec polarimetry has often provided evidence in favour of the interaction of these components with dense clouds of gas. For example, the southern component of 3C147 has a much higher RM than the northern component, is brighter, closer to the nucleus, and has the expected signatures of a jet colliding with a cloud of gas on the southern side of the galaxy (Junor et al. 1997). To explain both the low polarizations at centimeter wavelengths and the small linear sizes, it has been proposed that CSSs are cocooned in dense gaseous envelopes (e.g. Mantovani et al. 1994).

Existing ground-based optical observations show that narrow-line luminosities are comparable for CSSs and large-sized radio sources. However, broader narrow-line profiles found for CSSs suggest that the interaction of the jet with the ambient medium produces additional accelerations (Gelderman 1992; Morganti 1993; Gelderman & Whittle 1994). From the information available in the literature, it is not clear whether there is enough gas to support the so-called frustration scenario for CSSs, in which they are confined to small dimensions by dense interstellar media, thus hindering their evolution into classical FRII radio sources.

The structures of the sources shown here, with such large bent jets in the vicinity of the core, support the view of a strong interaction between the jet flow and dense gas clouds. This is in agreement with our estimate of the probability of having an interaction between the jet and a dense cloud of gas inside the first kpc from the nucleus. We predict that the widths of the narrow emission lines in these sources will be broader that for NLRGs (Narrow Line Radio Galaxies).

The interaction between the radio source and the ISM has been investigated, with time-dependent numerical simulations of jets associated with CSSs, by de Young (1993) in the following scenarios: *a)* the ISM is an uniform homogeneous medium, with a smooth density gradient; *b)* the ISM is in two phases — a hot tenuous gas together with a population of cold dense clouds; *c)* the interaction is with a single large feature such a very dense cloud. de Young shows that CSSs of low and intermediate luminosity can be confined by an ISM of average density 10 times that of the Galaxy. Confinement of the highest luminosity sources requires an ISM of unrealistic density and total mass. The population as a whole can be confined if the jets are intrinsically more efficient, by factors of 10 or more, than is commonly assumed for 'normal' radio sources.

The physics of jet-cloud collisions have been investigated by de Young (1991) and Norman & Balsara (1993) in 3-D hydro-dynamical simulations. Norman & Balsara do identify a fluid dynamical mechanism which maintains the collimation of the jet for all deflection angles $0° \leq \theta \leq 90°$. The reflected jet inherits the stability properties of the original jet. de Young shows that deflection of a jet in the case of jet-loud encounters over the short times ($\sim 10^6$ years) and distances (2 to 4 kpc) needed for CSSs may easily occur.

5. Conclusions

Fanti et al. (1995) have distinguished between double-lobed CSSs, which represent $\sim 70\%$ of the population and complex morphologied or asymmetric jet-dominated CSSs. They suggest that double-lobed CSSs represent the precursors of the large, double-lobed radio sources. The remaining 30% are sources with the jets brightened by Doppler boosting or by interaction with the ambient medium. The sources in Table 3 are classified as core-jet objects. The evidence that Doppler boosting can play a role in magnifying the large distortions seen in the jets is very weak. Radio structures, large RMs, and broader narrow line profiles support the view that large bent jets can be caused by interactions between the jets and dense gas clouds in the NLRs. Even a rough statistical computation indicates that the probability of a bump in the NLRs is statistically significant. 3-D hydrodynamical simulations of extragalactic jets reveal interesting features that further support this interpretation. In this picture, sources like 3C119 and 3C287 require more than one collision to createstructures that are spiral-like. Such cases cannot be excluded statistically, though they are very unlikely.

References

Alef W. & Preuss E. 1990 Proceedings *CSS & GPS Radio Sources*, Dwingeloo, eds. C. Fanti, R.Fanti, C.P. O'Dea and R.T. Schilizzi, p. 149

Barthel P. 1989 *ApJ* **336**, 606

van Bruegel, W.J.M., Miley, G & Heckman T. 1984 *A.J.* **89**, 5

van Bruegel, W.J.M., Fanti C. Fanti R. *et al.* 1992 *A&A* **256**,56

Cawthorne T., Wardle J.F.C., Roberts D.H. *et al.* 1993 *ApJ* **416**, 519

Conway J.E. & Murphy D.W. 1993 *Ap.J.*, **411**, 89

Cotton W.D. 1983 *Ap.J.*, **271**, 51

Cotton W.D., Owen F.N. & Geldzahler B.J. 1984 *Ap.J.* **277**,L41

Cotton W.D., Owen F.N., Mahoney M.J. 1989 *Ap.J.*, **338**, 37

Cotton W.D., Dallacasa D., Fanti C. et al. 1997 *A&A* in press

Cowie L. & Songaila A. 1896 *ARA&A*, **24**, 499

Cox D.P. & Reynolds R.J. 1987 *ARA&A*, **25**, 303

Dallacasa D. & Stanghellini C. 1990 *CSS & GPS Radio Sources*, Dwingeloo, eds. C. Fanti, R.Fanti, C.P. O'Dea & R.T. Schilizzi, p. 224

Dallacasa D., Fanti C., Fanti R. *et al.* 1995 *A&A* **295**, 27

Dallacasa D., Bondi M., Alef W. & Mantovani F. 1997 *A&AS* in press

de Young, D.S. 1991 *ApJ* **371**, 69

de Young, D.S. 1993 *ApJ* **402**, 95

Fanti, C. Fanti R. Schilizzi, R. T. *et al.* 1986 *A&A* **170**, 10

Fanti R., Fanti C. Schilizzi, R. T. *et al.* 1990, *A&A* **231**, 333

Fanti, C., Fanti R., Dallacasa D. *et al.* 1995 *A&A* **302**, 317

Fejes, I., Porcas R.W. & Akujor C.E. 1992 *A&A* **257**, 459

Garrington S. & Conway R. G. (1991) *MNRAS* **250**, 198

Garrington S. & Akujor C. E. 1996 *Extragalactic Radio Sources*, Bologna, eds. R. Ekers, C. Fanti & L. Padrielli, p. 77

Gelderman R. 1992 *Astrophysical Jets* eds. D. Bulgarella, M. Livio, & C.P. O'Dea (Cambridge University Press), p. 16

Gelderman R. & Whittle M. 1994 *ApJS* **91**, 491

Gopal-Krishna & Wiita, P.J. 1991 *AJ* **402**, 95

Kato T., Tabara H., Inoue M. & Aizu K. 1987 *Nature* **329**, 223

Kus, A. 1994 *Compact Extragalactic Radio Sources*, Socorro, New Mexico, eds. J. A. Zensus & K. I. Kellermann, p. 91

Junor, W., Salter, C.J., Saikia, D.J., *et al.* 1997 *Nature*, submitted

Laing R.A., Riley J.M., Longair M.S. 1983, *MNRAS* **204**,151

Mantovani F., Saikia D.J., Browne I.W. *et al.* 1990 *MNRAS* **245**,427

Mantovani F., Junor W., Fanti R. *et al.* 1992 *MNRAS* **257**, 353.

Mantovani, F., Junor, W., Fanti, R. *et al.* 1994 *A&A* **292**, 59

Mantovani, F., Junor, W., Fanti, R. *et al.* 1997 *A&AS*, **125**, 573

Marscher, A.P. & Shaffer, D.B. 1980 *A.J.*, **85**, 668

McCarthy, P.J. 1993 it A.R.A&A, **639**

Morganti R. 1993 *Sub-arcsecond Radio Astronomy* eds. Davis R. J. & Booth R. S., (Cambridge University Press)

Nan Ren-dong, Schilizzi R.T., Fanti, C. *et al.* 1991, *A&A* **245**, 449

Norman M.L. & Balsara D.S. 1993 *Jet in Extragalactic Radio Sources* eds. K. Meisenheimer & H.J. Roeser, Springer Verlag, Berlin, p. 229

O'Dea C.P., Baum S.A. & Morris G.B. 1990 *A&AS*, **82**, 261

Pearson T., Perley R.A. & Readhead A.C.S. 1985, *AJ* **90**, 738

Peacock J.A. & Wall J.V. 1982 *MNRAS* **198**, 843

Peterson B.M. 1997 *An Introduction to Active Galactic Nuclei*, Cambridge University Press, p. 101

Saikia, D. J. 1990 *CSS & GPS Radio Sources*, Dwingeloo, eds. C. Fanti, R.Fanti, C.P. O'Dea & R.T. Schilizzi, p.

Saikia, D.J., 1995 Proc. National Academy of Sciences, **vol. 92**, p. 11417

Saikia, D.J., Singal, A.K., Cornwell, T.J. 1987 *MNRAS* **224**, 379

Sanghera H.S., Saikia D.J., Lüdke E. *et al.* 1995 *A&A* **295**, 629

Shepherd M.C., Pearson T.J. & Taylor G.B., 1995 *BAAS* **26**, 987

Spencer R.S., Schilizzi R.T., Fanti C. *et al.* 1991 *MNRAS* **250**, 225

Spencer R.S. 1994 *Compact Extragalactic Radio Sources*, Socorro, New Mexico, eds. J. A. Zensus & K. I. Kellermann, p. 35

Spinrad H., Djorgovski S., Marr J. & Anguilar L. 1985 *Publs astr.Soc.Pacif.*, **97**,932

Stanghellini C., O'Dea C.P., Baum S.A. et al. 1993 *ApJS*, **88**, 1

Tabara H. & Inoue M. 1980 *A&A* **39** ,379

Taylor G.B., Inoue M. & Tabara H. 1992 *A&A* **264**, 421

Taylor G.B., Vermeulen R.C., Readhead A.C.S. *et al.* 1996 *AJSuppl.*, **107**, 37

Udomprasert P.S., Taylor G.B., Pearson T.J. & Roberts D.H. 1997, *ApJLetters*, in press

Venturi T., Pearson T.J., Barthel P.D. & Herbing T. 1993 *A&A* **271**, 65

Wilkinson, P.N., Akujor, C.E., Cornwell, T.J., Saikia, D.J., 1991 *MNRAS* **248**, 86

Wilkinson, P.N. 1995, *Quasars ans AGN: High Resolution Radio Imaging*, National Academy of Science Colloquium, Irvine, eds. M.H.Cohen & K.I. Kellermann, p. 11342